Investigation of 2D wind-borne debris in wind-tunnel and full-scale tests

Ning Lin[1], Chris W. Letchford[1] and John D. Holmes[2]
[1]Wind Science and Engineering Research Center, Texas Tech University, Lubbock, TX 79409, USA
[2]JDH Consulting, Mentone, Victoria, Australia

1. Introduction

Wind-borne debris is responsible for much damage in windstorms. The problem of debris may be summarized as one of flight initiation, flight speed (involving travel time and distance) and impact. Numerical modeling of the trajectory of windborne debris for incorporation in wind hazard risk assessment models requires knowledge of the aerodynamics of missiles. Experiments to determine the flight characteristics of rods (1D), plates (2D), and cubes and spheres (3D), were conducted in the Texas Tech University (TTU) wind tunnel. This paper presents the results of 2D debris from wind-tunnel tests and several full-scale tests employing a C130 Hercules aircraft.

2. Experiments

Tests were carried out in the closed circuit 1.8m wide by 1.2m high wind tunnel at Texas Tech University. The turbulence intensity varied from 0.5-3%. Twelve debris models ranging from 2.6 to 31.7 grams and 42mm to 150mm side lengths were studied. A circular electromagnet support (diameter b=18mm) was set at 0.6m high and 6.65 m in front of a catching net. Wind velocities were measured by a COBRA probe located adjacent to the magnet support. A digital video camera captured the flight trajectories. Full-scale tests were conducted with a Hercules C-130 aircraft to generate strong winds. Rectangular 4ft x 8ft plate debris ranging from 15 to 45 kg were launched from a 1m high table. Wind velocities were measured by a prop/vane anemometer located upstream of the launch table.

3. Results and Discussion

3.1 Trajectory of plates in the wind tunnel

The photographic records show the trajectory pattern of a plate depends mainly on its mode of motion, which in turn, is closely related to the initial angle of attack (θ). Fig. 1 shows, at different θ, the trajectories of square plate 4 (a, b), and rectangular plate 9 (D/B=0.42) (c, d) under low and high wind speeds. Tachikawa [1] defined three flight modes: auto-rotating, translatory and intermediate. Generally, at $\theta=0^0$ and 15^0, the plate entered into a clockwise auto-rotation and 'flies up' over a long distance and the trajectories for repeat trials were quite consistent. At $\theta=45^0$ and 90^0, the intermediate mode changes from clockwise to counter-clockwise rotation at initial stages of flight and to translatory at 45^0 to horizontal until hitting the ground. At $\theta=135^0$, with relatively low wind speed, one or two counter-clockwise rotations were followed by translatory motion similar to 45^0.

In addition to wind speed and initial angle of attack, the flight path of a plate depends on its geometry and support dimension and position. Fig. 2 (a) presents at $\theta=0^0$ the flight paths of plate 4 under wind speeds ranging from 8.5m/s to 20.8m/s. Fig. 2 (b) compares trajectories of the five square plates with K =6.7 ($K = \rho_a V_w^2 / 2tg\rho_m$, the ratio of aerodynamic force to gravity force, defined by Tachikawa [1] and Holmes [3]) and with similar values of $R_a = (B/b)^2$ (17-25). It is clear that the lift force increases with decreasing t/B and overcomes gravity to accelerate the plate into the air. As t/B increases eventually the flight path will approach that of 3D objects. To show the influence of the support dimension, trajectories of plate 4 and plate 1 with K=6.7 and with similar t/B (4-4.8%) values are compared in Fig.2 (c). The larger the ratio of plate area to support area, the larger is the initial lift force which increases the flight height. Since the initial situation affects the trajectory of plates, other support positions

were investigated. Fig. 2 (d) shows at $\theta=0^0$ and at a certain wind speed, the trajectories of plate 1 supported at the center, corner, and middle of the edge, respectively. When supported at the center of the plate, the lift force developed on the front half of the plate was largely unaffected by the support, however when supported in the middle of the plate front edge, gross disturbance to the flow occurs at the critical lift generation position making the plate fly poorly. However, these support effects were found to have relatively little influence on the maximum flight speed of plates.

3.2 Maximum velocities of plates in the wind tunnel

In order to study the impact of debris, it is necessary to predict the maximum velocities debris can attain within the region of interest. In the wind tunnel, at $\theta=0^0$, twelve plate models were tested with wind speeds ranging from 7.9m/s to 25.6m/s, until the plate hit the ceiling. Each test was repeated three to six times with differences between repeated trials typically less than 10%. Resultant and horizontal velocities were analysed for each trial. The maximum plate speeds were calculated by averaging all the repeated trial data using two calculation methods. The results are presented in Figs. 3 and 4.

The trajectories and speed of debris are conveniently expressed in non-dimensional terms. In the figures, α is the ratio of plate speed to wind speed, and α_m represents its maximum value. Tachikawa [1] defined a non-dimensional number $K = \rho_a V_w^2 / 2tg\rho_m$ for determination of the trajectory of debris. Fig. 3 (a) presents the α_m of cubes (3D) dependent on their K values. Even with different orientations, α_m values of 3D debris were well described by K. However, this parameter failed to describe the characteristics of 2D-debris, which is greatly influenced by geometry t/B and D/B. In Fig. 3(b), α_m of square plates falls into three layers. Basically, when t/B is 8.0-12.0% (plates 3, 5, and 6), α_m values range 0.55-0.65. When t/B is 4.0-5.0% (plates 1 and 4), most α_m values range 0.65-0.75. In the tests, most models were in these two layers. Wills et. al [2] also suggested 0.64 with a standard deviation of 0.1 for plates. However, when decreasing t/B to 2.8%, α_m of plate 8 could increase to over 0.9 (the third layer) before hitting the net 6.65m from the release position. Moreover, material density greatly affected α_m. Aluminium plate 7 with the smallest t/B (1.97%), fell into the lowest layer, while balsa plate 2 with medium t/B (4.7%) presented the highest α_m values of over 0.9 even at very low wind speeds. In Fig. 3 (c), similar tends with t/B can be observed for rectangular plates. The effect of side ratio D/B is also great. The larger the value of D/B, the smaller the value of α_m is obtained in the wind tunnel. Fig. 4 (a) presents results as the maximum observed rectangular plate speed versus wind tunnel speed.

To describe these features a non-dimensional parameter β is established based on a great deal of data:

$$\beta = (\frac{\rho_a}{\rho_m})^2 \frac{V_w^2}{2gt} \frac{B}{t} \sqrt{\frac{B}{D}} \quad (1)$$

The relationship of α_m with β is presented in Fig. 4 (b) for rectangular plates. These curves demonstrate a good empirical prediction of maximum plate speed at given wind speeds.

3.3 Full-scale tests

For the full-scale experiment, a Hercules C-130 aircraft was used to generate high wind events. Though having greater uncertainties, full-scale test results showed comparable flight behaviour with those in wind tunnel tests. Fig. 5 shows the trajectory of rectangular plate E1 (β=0.83) in the full-scale. The relationship of α_m and β for all full scale tests is shown in Fig. 6 and compares well with the relationship for wind tunnel results shown in Fig.4 (b).

4. Conclusions

2D debris models were investigated in both wind-tunnel and full-scale experiments. The characteristics (θ, t/B, D/B, ρ_m, V, support dimension and position) all affect the trajectories. A non-dimensional parameter β was established to describe the maximum 2D-debris speed

obtained in the wind-tunnel. Comparison of wind-tunnel and full-scale experiments shows reasonable agreement. With more data from wind tunnel tests, the empirical expression for maximum debris speed as a function of wind speed and 2D debris properties eq(1) can be further validated and used to estimate the flight speeds of potential debris around a structure. This data can then be employed in establishing rational debris impact criteria.

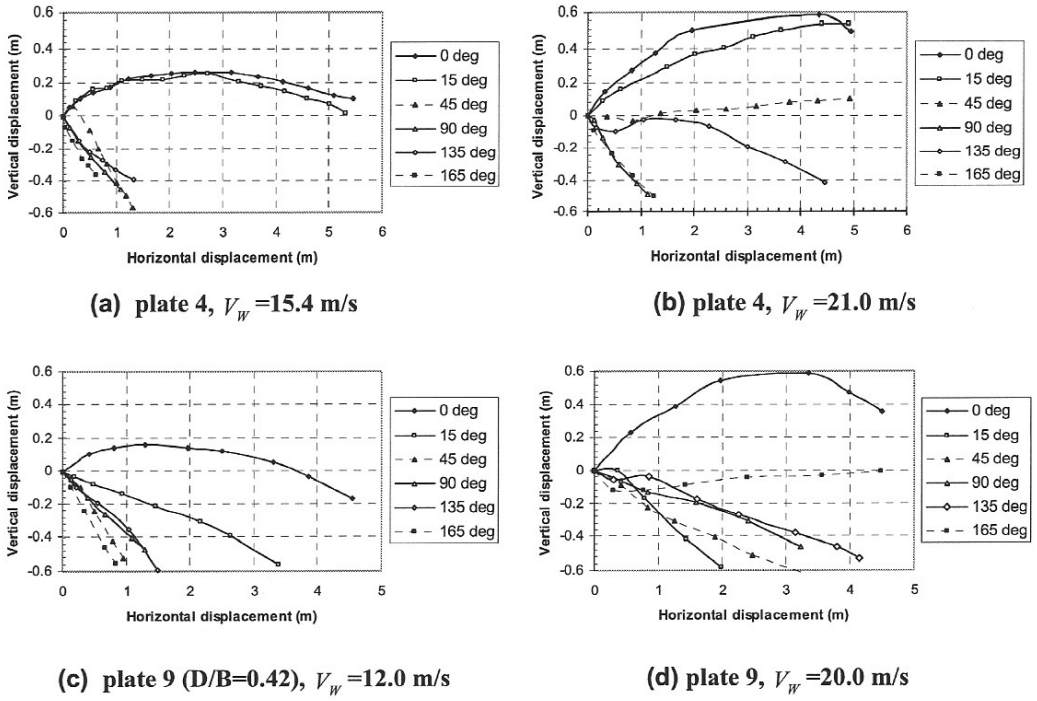

(a) plate 4, V_W =15.4 m/s

(b) plate 4, V_W =21.0 m/s

(c) plate 9 (D/B=0.42), V_W =12.0 m/s

(d) plate 9, V_W =20.0 m/s

Figure 1. Variations of trajectory and mode of motion with initial angle of attack θ

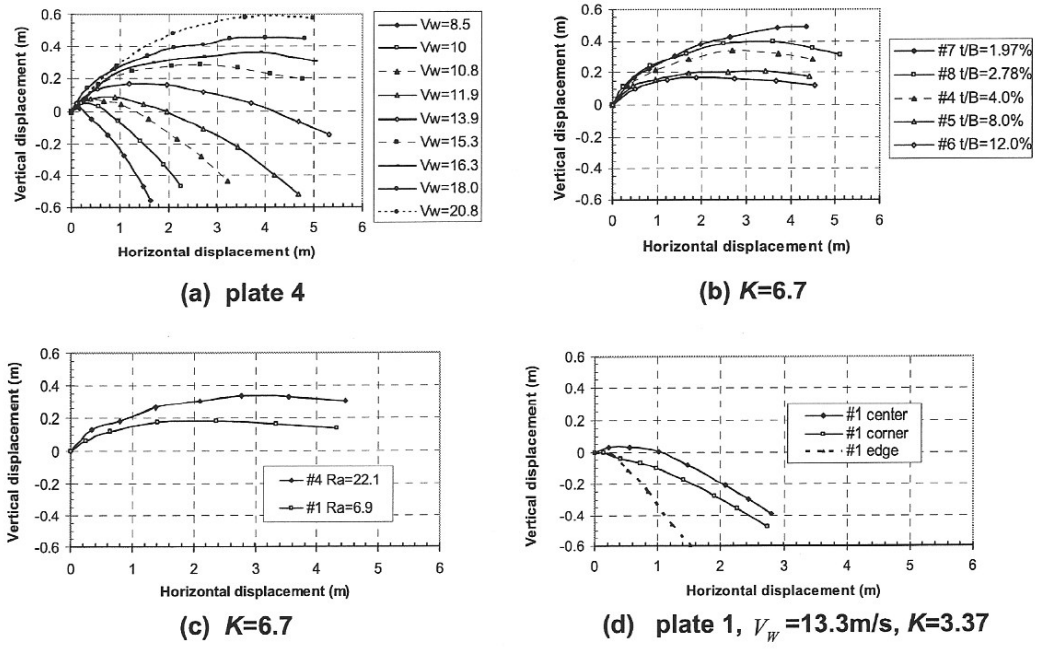

(a) plate 4

(b) *K*=6.7

(c) *K*=6.7

(d) plate 1, V_W =13.3m/s, *K*=3.37

Figure 2. Square-plate trajectories affected by (a) wind speed, (b) geometrical feature ($t/\sqrt{A}$), (c) ratio of plate area to support area (R_a), and (d) support location, at $\theta = 0^o$.

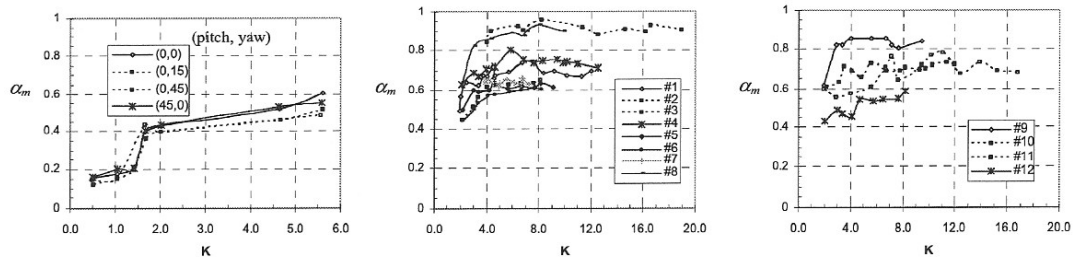

(a) cubes **(b) square plates** **(c) rectangular plates**

Figure 3. Non-dimensional maximum plate speed vs. K ($\theta = 0°$)

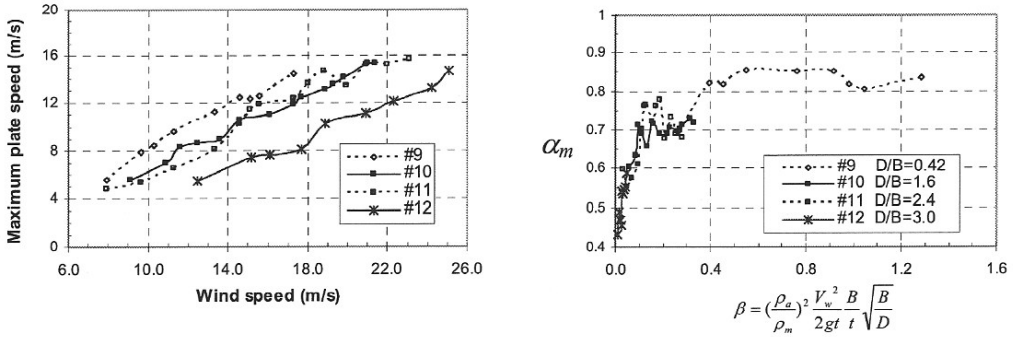

(a) maximum speed **(b) non-dimensional maximum speed vs. β**

Figure 4. Maximum speeds of rectangular plates in the wind tunnel ($\theta = 0°$)

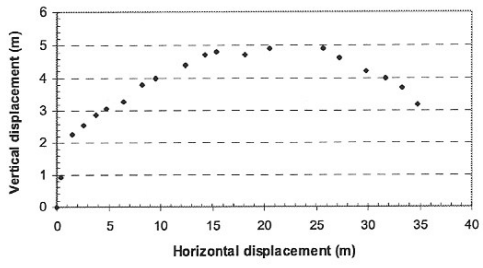

Figure 5. Trajectory of full scale plate E1 ($\beta = 0.83$, $\theta = 0°$)

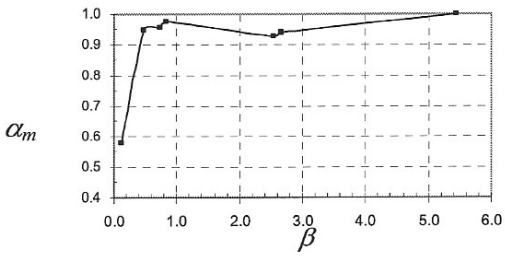

Figure 6. Non dimensional maximum speeds vs. β in full-scale tests ($\theta = 0°$)

5. Acknowledgements

This work was carried under the US Department of Commerce TTU/NIST Windstorm Mitigation Initiative. The assistance of Taylor Gunn, Dejiang Chen and Justin Miller in carrying out the plate tests and in providing data for cubes for comparison is gratefully acknowledged.

6. References

1. Tachikawa, M. (1983), Trajectories of flat plates in uniform flow with application to wind-generated missiles, *J. of Wind Engng and Ind. Aerodyn*, 14, 443-453
2. Wills, J.A.B., Lee, B.E. and Wyatt.T.A. (2002), A model of wind-borne debris, *J. of Wind Engng and Ind. Aerodyn,* 90, 555-565.
3. Holmes, J.D., (2004) Trajectories of spheres in strong winds with application to wind-borne debris, *J. of Wind Engng and Ind. Aerodyn,* 92, 9-22.